Distance-including rigorous upper bounds and tight estimates for two-electron integrals over long- and short-range operators

Travis H. Thompson, and Christian Ochsenfeld

Citation: The Journal of Chemical Physics **147**, 144101 (2017); doi: 10.1063/1.4994190
View online: http://dx.doi.org/10.1063/1.4994190
View Table of Contents: http://aip.scitation.org/toc/jcp/147/14
Published by the American Institute of Physics

Articles you may be interested in

Compressed representation of dispersion interactions and long-range electronic correlations
The Journal of Chemical Physics **147**, 144110 (2017); 10.1063/1.4997186

A study of accurate exchange-correlation functionals through adiabatic connection
The Journal of Chemical Physics **147**, 144105 (2017); 10.1063/1.4995698

Communication: Explicitly correlated formalism for second-order single-particle Green's function
The Journal of Chemical Physics **147**, 121101 (2017); 10.1063/1.5000916

Robust determination of the chemical potential in the pole expansion and selected inversion method for solving Kohn-Sham density functional theory
The Journal of Chemical Physics **147**, 144107 (2017); 10.1063/1.5000255

Connections between variation principles at the interface of wave-function and density-functional theories
The Journal of Chemical Physics **147**, 134107 (2017); 10.1063/1.4985883

An intrinsic representation of atomic structure: From clusters to periodic systems
The Journal of Chemical Physics **147**, 144106 (2017); 10.1063/1.4997292

Distance-including rigorous upper bounds and tight estimates for two-electron integrals over long- and short-range operators

Travis H. Thompson and Christian Ochsenfeld
Chair of Theoretical Chemistry, Department of Chemistry, University of Munich (LMU), Butenandtstr. 7, D-81377 Munich, Germany and Center for Integrated Protein Science Munich (CIPSM) at the Department of Chemistry, University of Munich (LMU), Butenandtstr. 5-13, D-81377 Munich, Germany

(Received 4 July 2017; accepted 5 September 2017; published online 9 October 2017)

We introduce both rigorous and non-rigorous distance-dependent integral estimates for four-center two-electron integrals derived from a distance-including Schwarz-type inequality. The estimates are even easier to implement than our so far most efficient distance-dependent estimates [S. A. Maurer *et al.*, J. Chem. Phys. **136**, 144107 (2012)] and, in addition, do not require well-separated charge-distributions. They are also applicable to a wide range of two-electron operators such as those found in explicitly correlated theories and in short-range hybrid density functionals. For two such operators with exponential distance decay [$e^{-r_{12}}$ and $\mathrm{erfc}(0.11 \cdot r_{12})/r_{12}$], the rigorous bound is shown to be much tighter than the standard Schwarz estimate with virtually no error penalty. The non-rigorous estimate gives results very close to an exact screening for these operators and for the long-range $1/r_{12}$ operator, with errors that are completely controllable through the integral screening threshold. In addition, we present an alternative form of our non-rigorous bound that is particularly well-suited for improving the PreLinK method [J. Kussmann and C. Ochsenfeld, J. Chem. Phys. **138**, 134114 (2013)] in the context of short-range exchange calculations. *Published by AIP Publishing.*
https://doi.org/10.1063/1.4994190

I. INTRODUCTION

Reducing the computational effort of quantum-chemical calculations requires taking advantage of the sparse nature of the interactions involved. This can be done efficiently through low-cost estimates that allow one to skip the exact calculation of numerically vanishing contributions. Traditionally, the development of reliable estimates of the four-center two-electron integrals over the Coulomb operator $1/r_{12}$ has played an important role in decreasing the storage and computational requirements. The use of the Schwarz estimate (QQ),

$$|(\mu\nu|\lambda\sigma)| \leq (\mu\nu|\mu\nu)^{1/2}\,(\lambda\sigma|\lambda\sigma)^{1/2} = Q_{\mu\nu}Q_{\lambda\sigma}, \quad (1)$$

where

$$(\mu\nu|\lambda\sigma) = \int\int \frac{\chi_\mu(\mathbf{r}_1)\chi_\nu(\mathbf{r}_1)\chi_\lambda(\mathbf{r}_2)\chi_\sigma(\mathbf{r}_2)}{r_{12}} d\mathbf{r}_1 d\mathbf{r}_2, \quad (2)$$

and $\{\chi_\mu\}$ is a finite set of sufficiently local orbitals (usually Gaussians), represents the first breakthrough in integral screening techniques.[1,2] It accurately captures the—in the case of Gaussian basis functions—exponential decay of two-electron integrals with increasing distances between the centers of χ_μ and χ_ν, and χ_λ and χ_σ (overlap dependence), while also being simple and very efficient to calculate.

More recently,[3] estimates have been developed that not only capture the overlap decay but also incorporate the decay of (2) arising from the behaviour of the Coulomb operator as the distance between the local charge distributions $\chi_\mu\chi_\nu$ and $\chi_\lambda\chi_\sigma$ becomes large (distance dependence). In this regard, Maurer *et al.* showed that a good approximation of the integrals can be even more useful than a strict upper bound and introduced the QQR estimate[3] given by

$$|(\mu\nu|\lambda\sigma)| \approx \begin{cases} Q_{\mu\nu}Q_{\lambda\sigma}(\tilde{R}^{\lambda\sigma}_{\mu\nu})^{-1}, & \tilde{R}^{\lambda\sigma}_{\mu\nu} > 1 \\ Q_{\mu\nu}Q_{\lambda\sigma}, & \tilde{R}^{\lambda\sigma}_{\mu\nu} \leq 1 \end{cases}, \quad (3)$$

where

$$\tilde{R}^{\lambda\sigma}_{\mu\nu} = R^{\lambda\sigma}_{\mu\nu} - \mathrm{ext}_{\mu\nu} - \mathrm{ext}_{\lambda\sigma}. \quad (4)$$

Here, $R^{\lambda\sigma}_{\mu\nu}$ is the distance between the centers of the two charge distributions $\chi_\mu\chi_\nu$ and $\chi_\lambda\chi_\sigma$, while $\mathrm{ext}_{\mu\nu}$ and $\mathrm{ext}_{\lambda\sigma}$ are their respective numerical extents (precise definitions in terms of entire shells are given in Ref. 3).

Further advances include the development of tighter estimates for three-center Coulomb integrals[4] and the extension of QQR to the operator $\mathrm{erfc}(\omega r_{12})/r_{12}$[5] used in some density functional theory (DFT) methods employing short-range exchange.

In the following, we introduce integral estimates that accurately describe the distance dependence and are applicable to a wide range of multiplicative, distance-dependent operators, including those that arise in some modern quantum-chemical methods, such as explicitly correlated F12[6,7] and short-range hybrid DFT methods.[8] The expressions are as simple and easily computable as the Schwarz estimates and are used to form both rigorous and even tighter non-rigorous estimates. In addition, they employ a distance-including term that is simpler and more efficient to calculate than that used in QQR type estimates. We test the estimates for integrals over the Coulomb operator $1/r_{12}$, which we call "long-range" due to their slow inverse distance decay, and over the operators $e^{-r_{12}}$ and $\mathrm{erfc}(0.11 \cdot r_{12})/r_{12}$, which we call "short-range" due to

their exponential distance decay. The operator $e^{-\gamma r_{12}}$ is important in explicitly correlated F12 theory with a true Slater-type geminal[9] and optimal values of γ depend on the basis set but are typically close to 1.0.[10] The operator $\mathrm{erfc}(0.11 \cdot r_{12})/r_{12}$ is used in, e.g., the HSE06,[11] HSE-3c,[12] and N12-SX[13] density functionals.

II. THEORY

The QQ estimate (1) remains applicable when the Coulomb operator $1/r_{12}$ is replaced by any positive-definite integral kernel, and in the following, we use the integral notation $(\mu\nu|\lambda\sigma)$ as in (2), but with the Coulomb operator replaced by some general function G of the inter-electronic distance. For proof of this statement and of the positive-definiteness of various important operators used in quantum chemistry, including those in this work, see Appendix B. Thus, from now on, the factor $Q_{\mu\nu}$ always depends implicitly on the operator G. In addition, we consider the generalized QQR estimate of the form

$$|(\mu\nu|\lambda\sigma)| \approx \begin{cases} Q_{\mu\nu}Q_{\lambda\sigma}G(\tilde{R}^{\lambda\sigma}_{\mu\nu}), & 0 < G(\tilde{R}^{\lambda\sigma}_{\mu\nu}) < 1 \\ Q_{\mu\nu}Q_{\lambda\sigma}, & \text{otherwise} \end{cases}, \tag{5}$$

with $\tilde{R}^{\lambda\sigma}_{\mu\nu}$ as in Eq. (4).

A. A rigorous upper bound for short-range operators

The QQ estimate is the Schwarz inequality on the space of one-electron charge distributions defined as $\Omega_{\mu\nu}(r_1) = \chi_\mu(r_1)\chi_\nu(r_1)$. It is applicable due to the fact that the two-electron integral over some distance-dependent operator G is an inner product on this space, as long as G is positive definite. We show in Appendix A that the integral is also an inner product on the space of real continuous two-electron functions, if G is strictly positive for $r_{12} > 0$. The two-electron orbital products $\tilde{\Omega}_{\mu\nu}(r_1, r_2) = \chi_\mu(r_1)\chi_\nu(r_2)$ are a subset of this space and the corresponding Schwarz inequality leads, due to symmetry, to the following two upper bounds:

$$|(\mu\nu|\lambda\sigma)| \le (\mu\mu|\lambda\lambda)^{1/2}\,(\nu\nu|\sigma\sigma)^{1/2} = M_{\mu\lambda}M_{\nu\sigma}, \tag{6}$$

$$|(\mu\nu|\lambda\sigma)| \le (\mu\mu|\sigma\sigma)^{1/2}\,(\nu\nu|\lambda\lambda)^{1/2} = M_{\mu\sigma}M_{\nu\lambda}. \tag{7}$$

In contrast to the original QQ estimates, the right-hand sides of (6) and (7) inherently contain distance dependence, while lacking any overlap dependence. Equality holds in (6) and (7) for integrals of type $(\mu\mu|\nu\nu)$, i.e., for "perfect" overlap in forming the charge distributions. We combine the original QQ estimates (1) and the Schwarz-type inequalities (6) and (7) into a rigorous distance-including upper bound, the combined Schwarz bound (CSB),

$$|(\mu\nu|\lambda\sigma)| \le \min\left(Q_{\mu\nu}Q_{\lambda\sigma}, M_{\mu\lambda}M_{\nu\sigma}, M_{\mu\sigma}M_{\nu\lambda}\right). \tag{8}$$

For the long-range Coulomb operator, overlap dependence is much more important than distance dependence and we find that the CSB estimate is no more useful than the QQ estimate for currently tractable systems. However, for operators with much stronger distance-decay, such as $e^{-r_{12}}$ and $\mathrm{erfc}(0.11 \cdot r_{12})/r_{12}$, we find that that the rigorous CSB provides a much tighter bound and correctly captures the linear scaling increase in the number of significant two-electron integrals already for medium-sized systems. This is in contrast to the QQ estimates, which scale quadratically with system size regardless of the operator, due to the missing distance-dependence.

Lastly, we note that the CSB estimates are exact for both $(\mu\nu|\mu\nu)$-type and $(\mu\mu|\nu\nu)$-type integrals. This is because the QQ estimates are exact for the former integral types, while Eqs. (6) and (7) are exact for the latter, and all three are upper bounds.

B. Tight estimates for short- and long-range operators

The descriptions provided by the QQ bounds and those in Eqs. (6) and (7) can be seen as being complementary. While the QQ estimates describe the overlap dependence at zero distance, the new bounds provide a description of the distance dependence at full overlap. This makes it plausible that they can be combined in a way that captures both properties simultaneously and gives a good estimate for most, if not all, of the two-electron integrals. In order to preserve the exactness of the estimates for $(\mu\nu|\mu\nu)$-type integrals, we developed the following normalized description of the distance decay:

$$\tilde{M}_{\mu\lambda} = \frac{M_{\mu\lambda}}{Q^{1/2}_{\mu\mu}Q^{1/2}_{\lambda\lambda}}. \tag{9}$$

We note that $0 < \tilde{M}_{\mu\lambda} \le 1$ and that $\tilde{M}_{\mu\lambda} = 1$ if $\chi_\mu = \chi_\lambda$. This follows from the QQ estimate of $M_{\mu\lambda}$,

$$M_{\mu\lambda} \le Q^{1/2}_{\mu\mu}Q^{1/2}_{\lambda\lambda}, \tag{10}$$

where equality holds if $\chi_\mu = \chi_\lambda$. The denominator in (9) depends neither on the overlap nor on the distance but ensures that the factor $\tilde{M}_{\mu\lambda}$ gives unity for $\chi_\mu = \chi_\lambda$ so that an estimate derived by multiplying the QQ bound with this factor will reduce to the QQ bound for $(\mu\nu|\mu\nu)$-type integrals, which is exact in this case. On the other hand, the distance decay of the factor $M_{\mu\lambda}$ is included. We use $\tilde{M}_{\mu\lambda}$ to formulate our non-rigorous combined Schwarz approximations (CSAs),

$$|(\mu\nu|\lambda\sigma)| \approx Q_{\mu\nu}Q_{\lambda\sigma}\mathcal{M}_{\mu\nu\lambda\sigma}, \tag{11}$$

with three different approximations [CSA1, CSA2, and CSA max (CSAM)] given by the choice of $\mathcal{M}_{\mu\nu\lambda\sigma}$,

$$\mathcal{M}_{\mu\nu\lambda\sigma} = \begin{cases} \tilde{M}_{\mu\lambda}\tilde{M}_{\nu\sigma}, & \text{CSA1} \\ \tilde{M}_{\mu\sigma}\tilde{M}_{\nu\lambda}, & \text{CSA2} \\ \max\left(\tilde{M}_{\mu\lambda}\tilde{M}_{\nu\sigma}, \tilde{M}_{\mu\sigma}\tilde{M}_{\nu\lambda}\right), & \text{CSAM} \end{cases}. \tag{12}$$

We note that in addition to $0 < \tilde{M}_{\mu\lambda} \le 1$, one also has

$$0 < \frac{Q_{\mu\nu}}{Q^{1/2}_{\mu\mu}Q^{1/2}_{\nu\nu}} \le 1, \tag{13}$$

with equality on the right-hand side for $\chi_\mu = \chi_\nu$, which follows by estimating $Q_{\mu\nu}$ with Eq. (6) [or (7)]. This ensures that the CSA estimates are also exact for integrals of type $(\mu\mu|\nu\nu)$ because they then reduce to the bound (6), which is exact in this case.

We note that CSA1 and CSA2 offer more flexibility due the separated form of $\mathcal{M}_{\mu\nu\lambda\sigma}$ but are slightly less accurate than CSAM (see Sec. III A). We have found, as one might expect, that CSA1 and CSA2 perform nearly identically and we only present results for CSA1.

The combined Schwarz approximations exhibit many excellent qualities. For one, they require only diagonal elements of the integrals themselves. Furthermore, no well-separatedness condition is required for their application, in contrast to QQR, and the error incurred in their use is mediated through only one screening parameter, the integral threshold. In addition, their use is very inexpensive because the distance factors $\tilde{M}_{\mu\nu}$ can be easily precalculated and stored, and only simple multiplication is needed in the screening step. Lastly, they lead, in terms of integral shell counts, to a nearly exact screening, i.e., the neglect of all integral shells with exact norms below the integral threshold, for all of the operators we have tested.

C. Incorporation into Coulomb and exchange matrix screening algorithms

Modern methods allow for the linear-scaling calculation of both the Coulomb (**J**) and exchange (**K**) matrices needed in Hartree-Fock (HF) theory and hybrid DFT (see, e.g., Ref. 14). **J** and **K** are defined in terms of the density matrix **P** and the two-electron integrals as

$$J_{\mu\nu} = \sum_{\lambda\sigma} P_{\lambda\sigma} (\mu\nu|\lambda\sigma), \tag{14}$$

$$K_{\mu\nu} = \sum_{\lambda\sigma} P_{\lambda\sigma} (\mu\lambda|\nu\sigma), \tag{15}$$

and traditionally, individual contributions are screened, i.e., contributions estimated below a chosen screening threshold are neglected, via the QQ bound,

$$|P_{\lambda\sigma} (\mu\nu|\lambda\sigma)| \leq |P_{\lambda\sigma}| Q_{\mu\nu} Q_{\lambda\sigma}, \tag{16}$$

$$|P_{\lambda\sigma} (\mu\lambda|\nu\sigma)| \leq |P_{\lambda\sigma}| Q_{\mu\lambda} Q_{\nu\sigma}. \tag{17}$$

In the case of the Coulomb matrix, the continuous fast multipole method (CFMM)[15] can be used to partition **J** into near-field and far-field contributions based on interaction distance. The near-field part inherently contains only a linear scaling number of interactions due to the distance cutoff and it is calculated using exact integrals, while the formally quadratic scaling far-field contribution is handled with arbitrary precision using a highly efficient multipole expansion based algorithm in a linear scaling fashion. Typically, the near-field contribution dominates Coulomb matrix calculation times and integral screening via Eq. (16) is used to reduce the prefactor.

The exchange matrix can be calculated in a linear scaling fashion for systems with non-vanishing HOMO-LUMO gaps, such that the density matrix **P** is sparse.[16–18] This is because the two charge distributions present in exchange terms are coupled through the density matrix as seen in (17) so that the number of significant contributions to **K** scales linearly in this case. Alternatively, very recent work[19] explores the use of fast multipole methods for calculating the exchange matrix.

While a naïve screening using Eq. (17) will scale quadratically with the system size, the LinK method[17,18] introduces a prescreening/preordering step preceding the Schwarz screening that reduces the complexity to linear for sparse **P** matrices.

We implement our estimates within the Coulomb near-field screening and LinK screening algorithms by simply adding a final screening step in which integrals are neglected when the estimates,

$$|P_{\lambda\sigma} (\mu\nu|\lambda\sigma)| \approx |P_{\lambda\sigma}| A_{\mu\nu\lambda\sigma}, \tag{18}$$

$$|P_{\lambda\sigma} (\mu\lambda|\nu\sigma)| \approx |P_{\lambda\sigma}| A_{\mu\lambda\nu\sigma}, \tag{19}$$

are less than some fixed thresholds ϑ_j and ϑ_k, for Coulomb and exchange contributions, respectively. Here, $A_{\mu\nu\lambda\sigma}$ represents one of the approximations to the two-electron integrals described above. Although one could tailor the prescreening step to the particular approximation used, we have found that this has little impact on the efficiency of calculating the exact exchange matrix, i.e., for two-electron integrals over the $1/r_{12}$ operator, to which this work is restricted. This is because the slow distance-decay allows for only small improvements in the coarse prescreening step. In addition, the large amount of non-negligible integrals means that the screening step makes up a small fraction of the calculation time in this case.

Lastly, we note that while the LinK prescreening algorithm is very efficient on central processing units (CPUs), it is not suited for use on graphical processing units (GPUs) due to the complex control flow required. However, the PreLinK prescreening method[20] allows for linear-scaling through a coarse preselection of significant **K** matrix elements before integral calculation begins using only efficient sparse matrix multiplications. Defining $|\mathbf{P}|$ as the matrix of absolute density matrix elements and **Q** as the matrix formed from the factors $Q_{\mu\nu}$, the approximated matrix of absolute exchange elements $|\mathbf{K}|'$ is given by the simple expression,

$$|\mathbf{K}|' = \mathbf{Q}|\mathbf{P}|\mathbf{Q}. \tag{20}$$

Because the CSB, QQR, and CSAM estimates do not separate into two-index quantities, they cannot be used straightforwardly within the PreLinK method because they do not lead to an efficient prescreening involving only matrix operations. On the other hand, the CSA1 estimates lead to a very simple expression for $|\mathbf{K}|'$,

$$|\mathbf{K}|' = \tilde{\mathbf{M}} \circ (\mathbf{Q}(\tilde{\mathbf{M}} \circ |\mathbf{P}|)\mathbf{Q}), \tag{21}$$

where $\circ$ symbolizes the Hadamard matrix product and $\tilde{\mathbf{M}} = (\tilde{M}_{\mu\nu})_{\mu\nu}$. Thus, only two Hadamard products and two matrix multiplications are required, which again can be performed in a linear-scaling fashion.

We have found that, in terms of speed vs. accuracy, Eq. (21) performs the same as (20) for the exact exchange calculations to which this work is restricted. This is not surprising considering the long-range nature of the $1/r_{12}$ operator and that the PreLinK method is a coarse prescreening. We note however that for short-range operators, the matrix $\tilde{\mathbf{M}}$ will become sparse for currently tractable systems and we have found Eq. (21) to perform significantly better than (20) in this case. Additionally, the sparsity of $\tilde{\mathbf{M}}$ means that for both the LinK and PreLinK methods, linear-scaling will be achievable even for small band-gap systems with densely populated density matrices. We will present results for short-range exchange calculations in future work.

III. COMPUTATIONAL DETAILS AND RESULTS

We compare the performance of the rigorous CSB [Eq. (8)] estimate and the non-rigorous CSA1 and CSAM [Eqs.

(11) and (12)] estimates to that of the established QQ [Eq. (1)] and QQR [Eq. (5)] estimates. For the QQR estimates, we employ a fixed well-separatedness threshold of 10^{-1}, which has been shown to give sufficient accuracy.[3] As test systems, we use a subset of the screening benchmark test suite described in Ref. 3.

In Sec. III A, preliminary results based on statistics and integral only screenings are given for the long-range Coulomb operator $1/r_{12}$ and the short-range operators $e^{-r_{12}}$ and $\mathrm{erfc}(0.11 \cdot r_{12})/r_{12}$. The importance of these operators is given at the end of Sec. I. We give results for a range of thresholds and also compare estimate performance for a series of linear alkanes containing up to 160 carbon atoms.

In Sec. III B, we give results for the $1/r_{12}$ operator in the context of Hartree-Fock SCF calculations to demonstrate the applicability of our estimates in electronic structure theory.

Due to the way in which molecular integrals are calculated, it is advantageous to screen at the level of integral shell-quartets. We estimate the contribution of a shell-quartet by taking the maximum norm of our estimates with respect to entire shells, before combining these shellwise estimates in the screening step to a final estimate. If a shell-quartet is deemed non-significant, none of the corresponding integrals are calculated.

A. Statistics and estimate performance

As a first test, we evaluate the performance of the estimates through statistics of the ratio

$$F = I_{\text{estimate}}/I_{\text{exact}}, \tag{22}$$

where I_{estimate} and I_{exact} are the estimated and actual norms of an integral shell-quartet, respectively. The maximum ($F_{\max}$), minimum ($F_{\min}$), average (F_{av}), and standard deviation [$\sigma(F)$] of F are given for the molecule Amylose_{16} from the test suite and the basis sets cc-pVDZ and cc-pVTZ in Tables I and II, respectively. Due to the way the integrals over the $\mathrm{erfc}(0.11 \cdot r_{12})/r_{12}$ operator are calculated as the difference between the integrals over the $1/r_{12}$ and $\mathrm{erf}(0.11 \cdot r_{12})/r_{12}$ operators, numerical instability occurs for large distances between charge distributions. Such integrals are calculated as the small difference between large values. As we show below, this does not affect the real performance of our estimates when using a fixed integral threshold; however, it distorts the statistics of F. To avoid this distortion, we restrict our statistics to shell-quartets with exact norms larger than 10^{-12}.

For the cc-pVDZ basis set we see, in the case of the $1/r_{12}$ operator, only slightly improved statistics with the CSB versus the QQ estimate. This is expected due to the weak distance dependence for this operator and we suspect that most of the improvement comes from $(\mu\mu|\nu\nu)$-type integrals for which CSB is exact while the QQ bounds are strict overestimates (assuming $\chi_\mu \neq \chi_\nu$). The non-rigorous QQR, CSAM, and CSA1 bounds perform similarly, with significantly improved averages, standard deviations, and maximal overestimates compared to the two rigorous bounds. The two CSA estimates have slightly improved standard deviations at a cost of slightly larger errors indicated by lower $F_{\min}$ values.

In the case of the $e^{-r_{12}}$ operator, the CSB estimate shows large improvements to the rather poorly performing QQ bound.

TABLE I. Statistics of the ratio $F = I_{\text{estimate}}/I_{\text{exact}}$ for the molecule Amylose_{16}, the cc-pVDZ basis set, and the estimates QQ, CSB, QQR, CSAM, and CSA1. Only shell-quartets with exact norms above 10^{-12} are included in the statistics.

cc-pVDZ					
Operator	Estimates	F_{av}	$\sigma(F)$	$F_{\min}$	$F_{\max}$
$1/r_{12}$	QQ	70.38	1.5×10^3	1.000	4.3×10^6
	CSB	62.06	954.00	1.000	2.3×10^6
	QQR	2.27	24.29	0.376	4.6×10^4
	CSAM	2.32	17.01	0.161	1.9×10^4
	CSA1	2.30	17.01	0.083	1.9×10^4
$e^{-r_{12}}$	QQ	1.4×10^6	2.0×10^7	1.000	7.3×10^9
	CSB	1.5×10^3	6.0×10^3	1.000	5.1×10^5
	QQR	12.76	47.45	0.179	1.6×10^4
	CSAM	2.39	6.20	0.002	1.3×10^3
	CSA1	1.88	4.97	2.4×10^{-4}	911.86
$\frac{\mathrm{erfc}(0.11 \cdot r_{12})}{r_{12}}$	QQ	2.0×10^6	4.0×10^7	1.000	3.9×10^{10}
	CSB	2.0×10^3	7.1×10^3	1.000	5.5×10^5
	QQR	5.14	5.49	0.448	741.05
	CSAM	1.48	1.30	0.042	132.70
	CSA1	1.34	1.22	0.014	125.33

Again, the non-rigorous estimates outperform the rigorous bounds greatly but come with the cost of underestimates which are more severe than in the case of the Coulomb operator. The CSA estimates are significantly better on average than the QQR estimates but also show much larger underestimates.

The results for the operator $\mathrm{erfc}(0.11 \cdot r_{12})/r_{12}$ are similar to those for $e^{-r_{12}}$. The non-rigorous estimates however show improved values in each category with the same general trends between them.

The results for the cc-pVTZ basis are very similar to those for the cc-pVDZ basis. The trends stay the same, but all

TABLE II. Statistics of the ratio $F = I_{\text{estimate}}/I_{\text{exact}}$ for the molecule Amylose_{16}, the cc-pVTZ basis set, and the estimates QQ, CSB, QQR, CSAM, and CSA1. Only shell-quartets with exact values above 10^{-12} are included in the statistics.

cc-pVTZ					
Operator	Estimates	F_{av}	$\sigma(F)$	$F_{\min}$	$F_{\max}$
$1/r_{12}$	QQ	101.54	2.6×10^3	1.000	9.0×10^6
	CSB	90.08	2.1×10^3	1.000	9.0×10^6
	QQR	3.05	43.28	0.337	9.9×10^5
	CSAM	3.15	30.06	0.145	3.4×10^4
	CSA1	3.12	30.06	0.069	3.4×10^4
$e^{-r_{12}}$	QQ	1.5×10^6	1.9×10^7	1.000	7.4×10^9
	CSB	1.8×10^3	8.1×10^3	1.000	1.2×10^7
	QQR	11.05	98.69	0.119	1.0×10^6
	CSAM	3.88	19.17	0.001	3.4×10^5
	CSA1	2.97	14.74	1.1×10^{-4}	2.2×10^5
$\frac{\mathrm{erfc}(0.11 \cdot r_{12})}{r_{12}}$	QQ	2.0×10^6	3.5×10^7	1.000	4.0×10^{10}
	CSB	2.3×10^3	8.6×10^3	1.000	6.5×10^6
	QQR	4.74	20.67	0.306	7.8×10^5
	CSAM	1.97	3.84	0.033	1.2×10^5
	CSA1	1.77	3.63	0.010	1.2×10^5

estimates perform slightly worse than with the smaller basis set.

We also present results regarding the efficiency and accuracy of direct integral screenings and compare to an *a posteriori* exact screening. In these tests, integrals are discarded when they are estimated to be smaller than a fixed threshold ϑ. In the case of the exact screening, they are discarded if they truly are smaller than the threshold. As a measure of the efficiency, we use significant shell-quartet totals, and as a measure of accuracy, the entrywise 1-norm (W) of the difference between the exact two-electron integral tensor $\{(\mu\nu|\lambda\sigma)\}$ and the "screened" tensor $\{(\mu\nu|\lambda\sigma)'\}$ with integrals from non-significant shell-quartets set to zero,

$$W = \sum_{\mu\nu\lambda\sigma} |\,(\mu\nu|\lambda\sigma) - (\mu\nu|\lambda\sigma)'\,|. \tag{23}$$

We note that W is just the unsigned sum of all discarded integral values. Although W will be much larger than the actual screening error due to error cancellation, it offers a good metric for comparison with the well-tested estimates QQ and QQR and with the error involved in an exact screening. We note that for non-rigorous methods, W will include contributions from integrals that are larger than the screening threshold; however, our accuracy metric treats such terms on equal footing with correctly discarded integrals, making a comparison with rigorous estimates possible. In almost all cases, the contribution from accurately screened integrals is larger or of the same order of magnitude as that coming from those discarded erroneously.

We tested our estimates using various screening thresholds. In Fig. 1, the ratio of the number of significant shell-quartets N_{SQ} of the most conservative ($\vartheta = 14$) QQ screening to those of each method/threshold (speedup) and the W values are plotted against a sequence of increasing screening thresholds ϑ for all three operators tested. The numbers are calculated using sums of the N_{SQ} and W data from the molecules Amylose_{32}, Polyethyne_{128}, and $(\text{S}_8)_{20}$ from the test suite.

For the $1/r_{12}$ operator [Figs. 1(a) and 1(d)], we find no improvement in efficiency for the rigorous CSB estimate and no change in accuracy compared to the QQ estimate. In fact, virtually identical sets of integrals are discarded in both cases. On the other hand, the non-rigorous estimates, which perform nearly identically, show significant improvements in efficiency close to that achieved with an exact screening. This increased speed is accompanied by an increase in error of more than an order of magnitude compared to the rigorous bounds. However the error is virtually identical to that of an exact screening and is controllable through the screening threshold. The error increases linearly with increasing ϑ.

In Fig. 1(b), we see that the speedups for the $\text{erfc}(0.11 \cdot r_{12})/r_{12}$ operator are much higher than for the $1/r_{12}$ operator for all estimates except QQ, for which they are more or less identical (notice the different scales for the speedup). Remarkably, the rigorous CSB estimate shows a speedup of ca. 2.5 already for $\vartheta = 10^{-14}$ with virtually no error increase. This can only be matched by the QQ estimate by increasing ϑ by six orders of magnitude, which is accompanied by an increase in error of roughly six orders of magnitude. The speedup gap between the two rigorous estimates increases with increasing ϑ, while the errors incurred [see Fig. 1(e)] remain virtually identical. Therefore, it seems that there can be no justification for the use of QQ instead of CSB for this operator. Looking at the non-rigorous estimates, we see speedups rivaling the exact screening from the CSA estimates with the QQR estimate discarding considerably less. The gap in speed between the non-rigorous and rigorous estimates has widened significantly in comparison to the $1/r_{12}$ operator. In contrast to the speedups, the errors of the screenings decrease across all estimates compared to the $1/r_{12}$ operator, especially for the QQ, QQR, and CSB estimates. This is notable considering the fact that many more integrals are discarded for this operator. One sees as well that the speedup of the CSA estimates compared to QQR comes at the price of a slight decrease in accuracy.

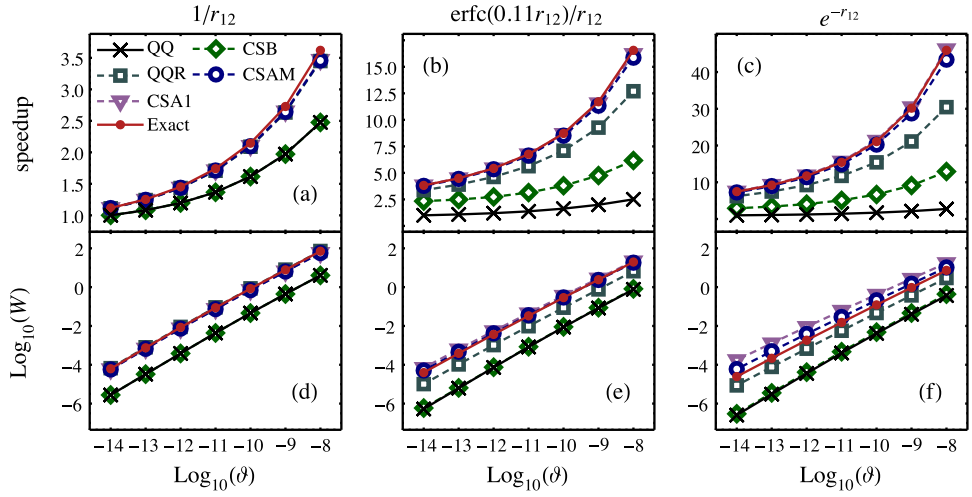

FIG. 1. [(a)-(c)] Speedup (relative to QQ estimates with screening threshold $\vartheta = 10^{-14}$) and [(d)-(f)] decadic logarithm of the error measure W [see Eq. (23)] for the molecular systems Amylose_{32}, Polyethyne_{128}, and $(\text{S}_8)_{20}$ for a series of screening thresholds ϑ. The number of significant shell-quartets and the W values are summed over the three molecules. The rigorous screenings QQ and CSB are compared to the non-rigorous QQR, CSAM, and CSA1 screenings as well as an *a posteriori* exact screening for the operators $1/r_{12}$ [(a) and (d)], $\text{erfc}(0.11 \cdot r_{12})/r_{12}$ [(b) and (e)], and $e^{-r_{12}}$ [(c) and (f)]. Note that while the range of speedup of the upper plots varies for the different operators, the range of the lower error plots is fixed.

The results for the $e^{-r_{12}}$ operator [Figs. 1(c) and 1(f)] are similar to that for $\mathrm{erfc}(0.11 \cdot r_{12})/r_{12}$, except that the speedups are much larger for all but the QQ estimates. Again, we find that CSB significantly outperforms the QQ estimates in efficiency with virtually no error penalty. We see the same trends between the non-rigorous estimates with a wider speed gap between the CSA and QQR estimates and between CSA1 and CSAM. The accuracy of the exact screening and rigorous estimates again increases, for QQR and CSAM it stays about the same, while the error of CSA1 increases slightly in comparison to the values for the $\mathrm{erfc}(0.11 \cdot r_{12})/r_{12}$ operator.

We also evaluated the performance of our estimates with increasing system size. In Fig. 2, the number of significant integral shell-quartets N_{SQ} and the W values are given for a set of linear alkanes ranging from methane to $C_{160}H_{322}$. Here, a fixed screening threshold of $\vartheta = 10^{-10}$ is used.

For the $1/r_{12}$ operator [Figs. 2(a) and 2(d)], we observe a quadratic increase in the number of significant shell-quartets with increasing system size for all estimates and for the exact screening, as expected. The non-rigorous estimates are nearly exact in terms of both significant shell-quartets and error.

For the $\mathrm{erfc}(0.11 \cdot r_{12})/r_{12}$ and $e^{-r_{12}}$ operators, we observe that all estimates except for QQ, including the rigorous CSB, correctly predict a linear scaling number of significant shell-quartets. While the CSB has an increased prefactor compared to the non-rigorous estimates, it shows almost no error increase compared to the QQ bound. Remarkably, for the largest alkane ($C_{160}H_{322}$), the QQ bound predicts 5.14 times as many significant shell-quartets as the CSB bound in the case of the $\mathrm{erfc}(0.11 \cdot r_{12})/r_{12}$ operator. For the $e^{-r_{12}}$ operator, this number increases to 8.09. The non-rigorous bounds are much closer to the exact screening in terms of significant integral shells. The CSA estimates are barely distinguishable from the exact screening, while the QQR estimate discards slightly less integrals. In terms of the accuracy of the non-rigorous estimates, CSA1 performs the worst in both cases, followed by CSAM and then QQR. We also note that the errors for all estimates and operators increase linearly with increasing system size.

In Sec. III B, we focus on the use of our newly introduced CSA estimates in Hartree-Fock SCF calculations, in which only the $1/r_{12}$ operator is needed. We will publish further results on the effectiveness of these estimates for the $\mathrm{erfc}(0.11 \cdot r_{12})/r_{12}$, $e^{-r_{12}}$, and other operators when integrated into the corresponding chemical theories in future work. For now, we point out that in these preliminary results, the errors of all estimates for the short-range operators $\mathrm{erfc}(0.11 \cdot r_{12})/r_{12}$ and $e^{-r_{12}}$ are lower than those seen for the QQR, CSAM, and CSA1 estimates for the $1/r_{12}$ operator. This is encouraging because, as shown in Ref. 3 for the QQR estimate and as we show in the following, these estimates can be well utilized in the efficient calculation of Coulomb and exchange matrices in SCF calculations of large molecules, while incurring minimal error. Thus we expect that our new estimates, CSB, CSAM, and CSA1, will perform very well for these and other operators when used in the respective theories.

B. Exact exchange SCF calculations

In the following, we present Hartree-Fock SCF calculations and compare the performance of the QQ bound with the QQR and our CSAM estimates. All calculations were run on 12 core CPU servers (2x Intel Xeon CPU E5-2620 @ 2.00 GHz). We use one screening threshold for exchange matrix integrals (ϑ_k) and a separate threshold (ϑ_j) for near-field Coulomb matrix integrals, which are calculated separately. Far-field Coulomb-type contributions are calculated using the CFMM[15] method for sufficiently large systems. As an SCF convergence criterion, the error calculated in the direct inversion of the iterative subspace method (DIIS error) is required to be below 10^{-7}, unless otherwise noted. The superposition of atomic densities is used as an initial guess.

We do not present results for the CSB bound because it performs identically to the QQ bound for the systems we tested. We expect that, for the $1/r_{12}$ operator, CSB will only perform

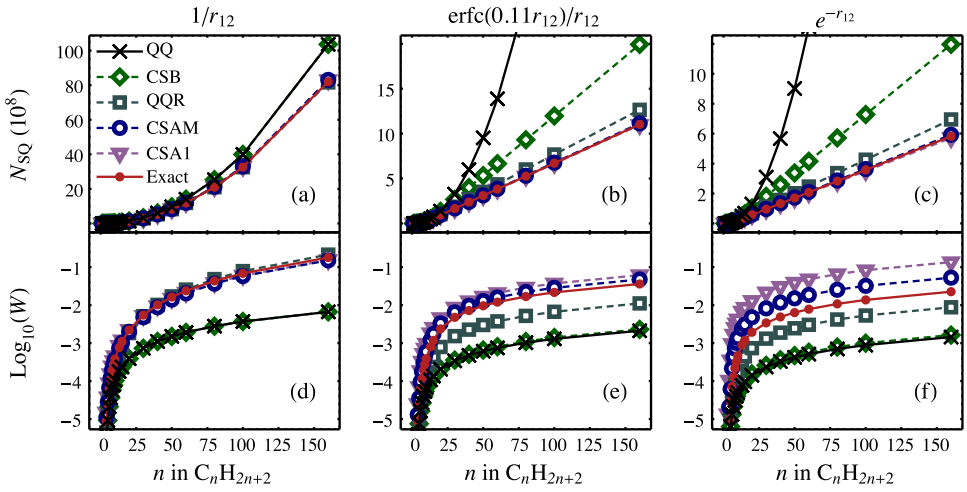

FIG. 2. [(a)-(c)] Number of significant shell-quartets (N_{SQ}) and [(d)-(f)] decadic logarithm of the error measure W [see Eq. (23)] for a series of linear alkanes of increasing length, five integral estimates, and the operators $1/r_{12}$ [(a) and (d)], $\mathrm{erfc}(0.11 \cdot r_{12})/r_{12}$ [(b) and (e)], and $e^{-r_{12}}$ [(c) and (f)]. The screenings were performed with a threshold of $\vartheta = 10^{-10}$ in all cases. Note that while the range of N_{SQ} in the upper plots varies for the different operators, the range of the lower error plots is fixed. In (b) and (c), some QQ points are omitted for large n for clarity. For the largest alkane ($n = 160$), the ratios of significant QQ to CSB shell-quartets are 5.14 and 8.09 for the $\mathrm{erfc}(0.11 \cdot r_{12})/r_{12}$ (b) and $e^{-r_{12}}$ (c) operators, respectively.

better than the QQ bound for unrealistically large systems. This is because of the slow distance-decay of the corresponding two-electron integrals.

1. Threshold dependence

As a first test of our CSA estimates for the Coulomb operator in the context of HF SCF calculations, we compare their performance for various screening thresholds. We vary the exchange screening threshold ϑ_k, while keeping the Coulomb matrix threshold ϑ_j fixed at $\vartheta_j = 10^{-12}$. In Fig. 3, we plot the decadic logarithm of the error vs. the computational time required in the SCF procedure, given as a percentage of the reference time. Here the molecule DNA_2 and the basis set cc-pVTZ were used. The error is calculated as the absolute difference between the converged energies of the reference calculation and the calculation performed with the respective estimates and thresholds. The exchange screening threshold varies from 10^{-9} (top left) to 10^{-12} (bottom right). The calculation with the QQ bound and $\vartheta_k = 10^{-12}$ is used as the reference and is shown as the dotted vertical line at the right of the plot. It has zero error by definition. Here, we see that the non-rigorous distance-including estimates perform much better than the QQ bound. They offer either improved speed with little loss of accuracy for a fixed threshold or vastly improved accuracy with the same calculation speed if used with a more conservative threshold. The exception is the QQR estimate with $\vartheta_k = 10^{-9}$, where four additional iterations are needed for SCF convergence, leading to no speedup compared to the QQ bound calculation with the same threshold. (The CSAM calculation with $\vartheta_k = 10^{-9}$ requires one additional SCF iteration, which can be attributed to small numerical differences.) CSAM gives very similar results to QQR with the exception of the just mentioned better convergence for $\vartheta_k = 10^{-9}$, causing it to be much faster with slightly less accuracy in this case. With $\vartheta_k = 10^{-10}$, CSAM is only slightly faster than QQR with a slight loss of accuracy, while for ϑ_k equal to 10^{-11} or 10^{-12}, it is slightly faster than QQR with no loss in accuracy.

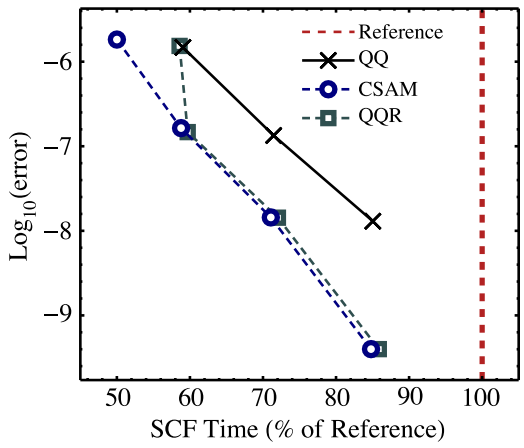

FIG. 3. Threshold dependence of the SCF calculations for the system DNA_2 and the basis set cc-pVTZ. Errors and SCF calculation times are given for the estimates QQ, QQR, and CSAM and exchange matrix integral thresholds ϑ_k varying from 10^{-9} (top left) to 10^{-12} (bottom right), with the combination QQ/10^{-12} used as the reference. The Coulomb matrix integrals are screened with a constant threshold $\vartheta_j = 10^{-12}$. The error is given as the unsigned difference between the converged energies of the reference and the respective estimate/threshold combinations.

2. System and basis set dependence

In the following, we give results for a wide range of chemical systems from the screening test suite and three different basis sets. For each estimate and system tested, we give errors and speedups with respect to reference calculations.

Unless otherwise noted, the calculations are performed with Coulomb and exchange integral thresholds of

TABLE III. Errors (E) and speedups (SU) with respect to reference calculations for HF SCF calculations and the cc-pVDZ basis set. The calculations are performed with $\vartheta_j = \vartheta_k = 10^{-10}$ unless noted otherwise. References are calculated with the QQ estimate and $\vartheta_j = \vartheta_k = 10^{-12}$.

cc-pVDZ basis set						
	QQ		QQR		CSAM	
System	E (μH)	SU	E (μH)	SU	E (μH)	SU
$Amylose_2$	−0.02	1.28	−0.02	1.30	−0.05	1.43
$Amylose_4$	−0.04	1.34	−0.06	1.48	−0.12	1.60
$Amylose_8$	−0.09	1.50	−0.13	1.76	−0.26	1.84
$Amylose_{16}$	−0.19	1.53	−0.27	1.88	−0.54	1.97
$Amylose_{32}$	−0.39	1.57	−0.57	1.88	−1.16	1.98
$Amylose_{48}$	−0.60	1.55	−0.86	1.88	−1.74	1.99
$Amylose_{64}$	−0.80	1.56	−1.14	1.88	−2.32	1.97
Angiotensin	−0.10	1.50	−0.12	1.72	−0.19	1.85
Angiotensin dep.	−0.10	1.50	−0.12	1.74	−0.18	1.87
Angiotensin zw.	−0.10	1.49	−0.13	1.73	−0.18	1.83
CNT_{20}[a]	−0.02	1.18	−0.01	1.17	−0.06	1.24
CNT_{40}[a]	−0.07	1.28	−0.13	1.33	−0.24	1.41
CNT_{80}[a]	−0.22	1.36	−0.31	1.48	−0.44	1.55
$CNT(6,3)_8$[a]	−4.18	1.76	−6.70	2.74	−9.35	2.78
$Diamond_{102}$	−0.20	1.35	−0.37	1.45	−1.70	1.55
DNA_1	−0.03	1.29	−0.03	1.39	−0.06	1.48
DNA_2	−0.13	1.49	−0.15	1.71	−0.23	1.82
DNA_4	−0.33	1.62	−0.41	2.03	−0.56	2.15
DNA_8	−0.71	1.79	−0.92	2.46	−1.25	2.57
DNA_{16}	−1.49	1.92	−1.88	2.74	−2.62	2.81
$Graphite_{24}$	−0.02	1.23	−0.04	1.28	−0.05	1.34
$Graphite_{54}$	−0.15	1.32	−0.25	1.42	−0.34	1.49
$Graphite_{96}$	−0.35	1.37	−0.68	1.54	−0.91	1.61
$(H_2O)_{68}$	−0.08	1.74	−0.05	2.19	0.03	2.32
$(H_2O)_{142}$	−0.23	1.88	−0.14	2.59	0.13	2.72
$(H_2O)_{285}$	−0.54	2.10	−0.27	3.04	0.39	3.19
$(H_2O)_{569}$	−1.17	2.30	−0.55	3.55	0.98	3.70
$(LiF)_{32}$	−0.02	1.13	−0.10	1.18	−0.13	1.20
$(LiF)_{72}$	0.09	1.19	−0.65	1.25	−0.60	1.29[b]
Phtalocyanine c.	−0.05	1.25	−0.09	1.34	−0.16	1.40
$Polyethyne_{64}$	−0.02	1.34	−0.02	1.71	−0.07	1.73
$Polyethyne_{128}$	−0.04	1.44	−0.05	1.91	−0.15	1.92
$Polyyne_{64}$	0.04	1.14	−0.54	1.30[c]	−0.05	1.31
$Polyyne_{1024}$[d]	0.67	1.20	−0.01[e]	1.28[c,e]	0.74[e]	1.31[e]
$(S_8)_5$	−0.10	1.37	−0.10	1.53	−0.09	1.66
$(S_8)_{20}$	−0.54	1.66	−0.45	2.19	−0.29	2.36
Triphenylmethyl	−0.01	1.23	−0.02	1.28	−0.05	1.34

[a]Convergence criterion relaxed to DIIS error below 10^{-6}.
[b]One less SCF iteration than reference calculation required.
[c]One more SCF iteration than reference calculation required.
[d]Convergence criterion relaxed to DIIS error below 10^{-5}.
[e]$\vartheta_j = 10^{-11}$, $\vartheta_k = 10^{-12}$.

$\vartheta_j = \vartheta_k = 10^{-10}$, while the reference calculations are performed with the QQ bound and $\vartheta_j = \vartheta_k = 10^{-12}$.

In Table III, we give the results for the cc-pVDZ basis set for a wide range of chemical systems. The errors (E) are given as differences in converged energies compared to the reference in microhartree (μH), while the speedups (SU) are given as the ratios of the sum of Coulomb and exchange matrix computation times (using the converged density) to that of the reference. In general, the errors are roughly proportional to the system size for each estimate. For almost all systems, the speedups are the lowest with the QQ screening and highest using our CSAM. The only exception is for the CNT_{20} molecule for which QQR is slightly slower than QQ. In some cases (see footnotes of Table III), the calculations using the QQR estimate require an additional SCF iteration for convergence, while in one case [$(LiF)_{72}$] the calculation with CSAM requires one less iteration than the reference. Typically, the size of the errors increases when going from QQ to QQR and from QQR to CSAM. The H_2O and S_8 clusters are exceptions to this rule; here, the non-rigorous bounds give energies closer or just as close to the reference. Most importantly, we find small absolute errors for all of the estimates and systems tested. The largest errors occur for the sizeable $CNT(6,3)_8$ molecule, with absolute errors of 4.18, 6.70, and 9.35 μH with the QQ, QQR, and CSAM estimates, respectively. For all but the largest systems, errors of below 2 μH are observed.

In Table IV, we present analogous results for the cc-pVTZ basis set and smaller subset of the test suite. For this larger basis set, we see increased speedups and typically a larger gap between QQ and the non-rigorous estimates compared to the same systems with a smaller cc-pVDZ basis set. There is almost no speedup gap between QQR and CSAM for this basis set and CSAM is only marginally faster in most cases. Interestingly, the errors incurred using the QQ bound typically increase using the larger basis set, while those of the QQR estimate are not significantly different and those of the CSAM estimate typically decrease. This leads to errors that are very similar across screening methods. Often the CSAM gives less error than QQR, while still being slightly faster. The largest absolute errors are only 1.02 μH ($Graphite_{54}$, CSAM) and 1.01 μH ($Polyyne_{64}$, QQR).

TABLE IV. Errors (E) and speedups (SU) with respect to reference calculations for HF SCF calculations and the cc-pVTZ basis set. The calculations are performed with $\vartheta_j = \vartheta_k = 10^{-10}$. References are calculated with the QQ estimate and $\vartheta_j = \vartheta_k = 10^{-12}$.

	cc-pVTZ basis set					
	QQ		QQR		CSAM	
System	E (μH)	SU	E (μH)	SU	E (μH)	SU
$Amylose_8$	−0.10	1.59	−0.11	2.02	−0.12	2.05
Angiotensin	−0.12	1.57	−0.14	1.99[a]	−0.12	2.01[a]
Angiotensin dep.	−0.13	1.59	−0.15	1.98	−0.13	2.01
Angiotensin zw.	−0.12	1.60	−0.15	2.01[a]	−0.12	2.03
CNT_{40}[b]	−0.10	1.33[a]	−0.16	1.44	−0.22	1.49[a]
$Diamond_{102}$	−0.31	1.43	−0.99	1.61[a]	−0.97	1.67
DNA_2	−0.14	1.54	−0.20	1.89	−0.17	1.92
$Graphite_{54}$	−0.22	1.34[a]	−0.38	1.51[c]	−1.02	1.54[c]
$(H_2O)_{68}$	−0.12	1.85	−0.22	2.53	−0.25	2.54
$(LiF)_{32}$	−0.02	1.18	0.02	1.27	0.02	1.27
$Polyyne_{64}$	−0.50	1.18	−1.01	1.42	−0.13	1.42
$(S_8)_{20}$	−0.46	1.72	−0.26	2.33	0.38	2.42
Triphenylmethyl	−0.02	1.29	−0.04	1.38[d]	−0.06	1.42

[a]One more SCF iteration than reference calculation required.
[b]Convergence criterion relaxed to the DIIS error below 10^{-6}.
[c]Two more SCF iterations than reference calculation required.
[d]One less SCF iteration than reference calculation required.

TABLE V. Errors (E) and speedups (SU) with respect to reference calculations for HF SCF calculations and the aug-cc-pVDZ basis set. The calculations are performed with $\vartheta_j = \vartheta_k = 10^{-12}$. References are calculated with the QQ estimate and $\vartheta_j = \vartheta_k = 10^{-14}$.

	aug-cc-pVDZ basis set					
	QQ		QQR		CSAM	
System	E (nH)	SU	E (nH)	SU	E (nH)	SU
$Amylose_8$	−0.40	1.21	1.40	1.33	−0.20	1.34
Angiotensin	−1.50	1.18	−1.80	1.25	1.80	1.29
DNA_2	−0.50	1.19	−2.60	1.26	−0.80	1.27
$(H_2O)_{68}$	0.70	1.35	−6.80	1.53	−0.80	1.52
$(LiF)_{32}$	−0.10	1.06	0.70	1.08	1.00	1.09
Triphenylmethyl	−0.20	1.06	−0.30	1.06	−0.10	1.09

In Table V, we give results for a basis set augmented with diffuse basis functions, the aug-cc-pVDZ basis set. In this case, tighter thresholds are required to ensure SCF convergence regardless of the estimate used and thus we choose Coulomb and exchange integral thresholds of $\vartheta_j = \vartheta_k = 10^{-12}$, with reference calculations using the QQ bound and $\vartheta_j = \vartheta_k = 10^{-14}$. Due to the tighter thresholds, the speedups are less than seen for the previous two basis sets. On the other hand, the errors are reduced drastically and are now given in nanohartree (nH). The speedups of the QQR and CSAM estimates are largely similar, with CSAM marginally faster than QQR for all but one system [$(H_2O)_{68}$]. CSAM outperforms QQR in accuracy for all but two systems [angiotensin, $(LiF)_{32}$].

IV. CONCLUSION AND OUTLOOK

We have presented first results for our newly developed distance-including rigorous bound CSB and non-rigorous estimates CSA for three different operators [$1/r_{12}$, $\mathrm{erfc}(0.11 \cdot r_{12})/r_{12}$, and $e^{-r_{12}}$] based on direct integral screenings that are independent of any quantum-chemical theory. In addition we have implemented the CSA estimates in the context of Hartree-Fock SCF calculations and shown that they can be used to speed up integral calculation compared to both the distance-neutral QQ bound and distance-including QQR estimates. The errors incurred are, in almost every case, of the same order of magnitude as for the QQ and QQR estimates and are controllable through the chosen screening threshold.

We expect, based on the results in Sec. III A, that the CSB bound and CSA estimates will perform even better in comparison to the QQ and QQR estimates for operators with much stronger distance-decay than the $1/r_{12}$ Coulomb

operator. In fact, one could already consider CSB as the new default estimate for short-range operators due to its rigorous nature, ease of implementation, low cost, and vastly superior performance compared to the QQ bound. On the other hand, the CSAM estimate has several advantages over the QQR estimate that become more pronounced for short-range operators. One of these advantages is the near-exact nature of the estimate for the short-range operators that we have tested. Another is the fact that the screening itself can be performed more efficiently because the distance-including factor is calculated through two multiplications and one logical operation, whereas in QQR the distance between shell-pairs must be calculated and inserted into an operator function that is relatively expensive to compute. This extra cost is also more important for short-range operators because the ratio of screening time to integral calculation time will naturally go up due to the much larger numbers of insignificant integrals. Regarding the CSA1 estimate, it remains to be seen how it will perform when used in the PreLinK method for short-range exchange DFT calculations. We will compare it to the QQ bound and other distance-including PreLinK methods[5] in this context in future work.

ACKNOWLEDGMENTS

The authors thank Dr. Jörg Kussmann (LMU Munich) for valuable suggestions for improving the manuscript.

Financial support by the DFG funding initiatives Oc35/4-1 and SFB749 (C7) and the Excellence Cluster EXC114 (CIPSM) is acknowledged.

APPENDIX A: PROOF OF EQS. (6) AND (7)

We first prove a more general statement for any pair of two-electron functions. We denote with $\mathcal{E}_2$ the real vector space of all continuous real-valued functions of the positions of two-electrons. We consider the two-electron integral with multiplicative operator G as a map $\langle\cdot,\cdot\rangle$ from the product space $\mathcal{E}_2 \times \mathcal{E}_2$ onto the real numbers,

$$\langle e,f\rangle = \int\int e(r_1,r_2)G(r_{12})f(r_1,r_2)dr_1dr_2\,, \tag{A1}$$

where e and f are functions in $\mathcal{E}_2$, and show that $\langle\cdot,\cdot\rangle$ defines an inner product on $\mathcal{E}_2$. We assume that $G(r_{12})$ is positive for $r_{12} > 0$ (positivity property). In order for $\langle\cdot,\cdot\rangle$ to be an inner product, it must satisfy the following requirements for any functions e, f, g in $\mathcal{E}_2$ and any real number λ:

1. $\langle e,f\rangle = \langle f,e\rangle$,
2. $\langle \lambda e,f\rangle = \lambda\langle e,f\rangle$,
3. $\langle e+g,f\rangle = \langle e,f\rangle + \langle g,f\rangle$,
4. $\langle e,e\rangle \geq 0$,
5. $\langle e,e\rangle = 0$ if and only if $e \equiv 0$.

The first requirement follows from the fact that G is multiplicative, while requirements two and three follow from the linearity of integrals. To show four and five, we note the fact that the value of the integral (A1) does not change when we restrict the integration to values of r_1 and r_2, such that $r_{12} \neq 0$. Therefore, we have, using the multiplicity and positivity property of G, that

$$\langle e,e\rangle = \int\int e^2(r_1,r_2)G(r_{12})dr_1dr_2 \geq 0 \tag{A2}$$

because the integrand is always positive for $r_{12} \neq 0$. This is requirement four. If $e(r_1, r_2)$ does not vanish for some pair of positions (r_1, r_2), then the continuity of e and the positivity property of G dictate that $\langle e,e\rangle > 0$ must hold. On the other hand, if e vanishes for all possible (r_1, r_2), then $\langle e,e\rangle$ must be zero. These two facts together are requirement five and this ends the proof that $\langle\cdot,\cdot\rangle$ is an inner product.

Because $\langle\cdot,\cdot\rangle$ is an inner product, the Schwarz inequality for any two functions e, f in $\mathcal{E}_2$ holds,

$$\langle e,f\rangle \leq \langle e,e\rangle^{1/2}\langle f,f\rangle^{1/2}\,, \tag{A3}$$

with equality if and only if e and f are linearly dependent. Equations (6) and (7) are a direct consequence of (A3) when e and f are replaced by the corresponding products of Gaussian basis functions (and Mulliken integral notation is used).

APPENDIX B: A NOTE ON THE APPLICABILITY OF THE SCHWARZ INEQUALITY (QQ BOUND) TO INTEGRALS OVER MULTIPLICATIVE, DISTANCE BASED OPERATORS

Proofs for the Schwarz inequality for two-electron integrals over the Coulomb operator $1/r_{12}$ have appeared in various forms in the quantum chemical literature[1,21,22] and more general theorems can be found in mathematical physics textbooks, see, for example, Refs. 23 and 24. Although the inequality has been used, as in this work, for two-electron integrals over other operators,[25,26] this has been done without giving explicit proofs or references to proofs for these cases. We have also been unable to find explicit proofs elsewhere in the literature. Thus, in this section, we aim to clarify the applicability of the Schwarz inequality by giving a simple, sufficient condition for any multiplicative, distance based operator. Our condition is based on the proof for the Coulomb operator given in Ref. 22. Further, we show explicitly that this condition is met not only for the operators used in this work but also for some other important operators in quantum chemical theories.

Let G be some multiplicative operator depending on the distance between the positions of two electrons. In order to show that

$$|\,(\mu\nu|_G|\lambda\sigma)\,| \leq (\mu\nu|_G|\mu\nu)^{1/2}\,(\lambda\sigma|_G|\lambda\sigma)^{1/2}\,, \tag{B1}$$

where

$$(\mu\nu|_G|\lambda\sigma) = \int\int \chi_\mu(\mathbf{r}_1)\chi_\nu(\mathbf{r}_1)G(\mathbf{r}_1-\mathbf{r}_2) \times \chi_\lambda(\mathbf{r}_2)\chi_\sigma(\mathbf{r}_2)d\mathbf{r}_1d\mathbf{r}_2, \tag{B2}$$

it suffices to show that the integral $(\mu\nu|_G|\lambda\sigma)$ defines an inner product on the space spanned by all the orbital products $\chi_\mu\chi_\nu$. For this, the same conditions given in Appendix A, with e, f, and g replaced by one-electron functions, must be fulfilled. Again, the first three conditions follow directly from the

multiplicativity of G and the linearity of the integral. However, conditions four and five turn out to be slightly more difficult to show, due to the fact that the integrand on the right-hand side of the equation,

$$(f|f) = \int\int f(\mathbf{r}_1)f(\mathbf{r}_2)G(\mathbf{r}_1 - \mathbf{r}_2)d\mathbf{r}_1 d\mathbf{r}_2, \tag{B3}$$

is not everywhere positive. Here f is any one-electron function for which (B3) converges. Assuming G has a well-defined three-dimensional Fourier transform $\mathcal{F}_G$, given by

$$\mathcal{F}_G(k) = \frac{1}{2\pi}\int G(\mathbf{r})e^{-i\mathbf{k}\cdot\mathbf{r}}d\mathbf{r}, \tag{B4}$$

we can represent G in terms of its inverse Fourier transform,

$$G(\mathbf{r}) = \int \mathcal{F}_G(k)e^{i\mathbf{k}\cdot\mathbf{r}}d\mathbf{k}. \tag{B5}$$

Here we write $\mathcal{F}_G$ as a function of $k = |\mathbf{k}|$, which is possible because G only depends on $r = |\mathbf{r}|$. This allows us to write (B3) as

$$(f|f) = \int \mathcal{F}_G(k)|\tilde{f}(\mathbf{k})|^2 d\mathbf{k}, \tag{B6}$$

where

$$\tilde{f}(\mathbf{k}) = \int f(\mathbf{r})e^{-i\mathbf{k}\cdot\mathbf{r}}d\mathbf{r}. \tag{B7}$$

Thus, when $\mathcal{F}_G$ has the positivity property defined in Appendix A, the same arguments given there apply in this case so that conditions four and five follow analogously, and the Schwarz inequality can be used with the operator G. The condition $\mathcal{F}_G(k) > 0$ for $k > 0$ is, according to Bochner's theorem,[27] equivalent to the statement that G is a positive-definite function.

It thus suffices to calculate the Fourier transform of G and check that it is positive for $k > 0$. This can be done, e.g., using the following formula of Grafakos and Teschl:[28]

TABLE VI. Fourier transforms for some important operators in quantum chemical theories. The parameters γ, ω, and α are positive real numbers. All transforms are strictly positive for $k > 0$.

Operator	Fourier transform
$1/r_{12}$	$\frac{1}{2\pi^2 k^2}$
$e^{-\gamma r_{12}}$	$\frac{\gamma}{\pi^2(k^2+\gamma^2)^2}$
$e^{-\gamma r_{12}}/r_{12}$	$\frac{1}{2\pi^2(k^2+\gamma^2)}$
$\mathrm{erf}(\omega r_{12})/r_{12}$	$\frac{1}{2\pi^2 k^2}e^{-\frac{k^2}{4\omega^2}}$
$\mathrm{erfc}(\omega r_{12})/r_{12}$	$\frac{1}{2\pi^2 k^2}(1 - e^{-\frac{k^2}{4\omega^2}})$
$e^{-\alpha r_{12}^2}$	$\frac{1}{8\pi^{3/2}\alpha^{3/2}}e^{-\frac{k^2}{4\alpha}}$

$$\mathcal{F}_G(k) = -\frac{1}{2\pi k}\frac{d}{dk}\tilde{\mathcal{F}}_G(k), \tag{B8}$$

where $\tilde{\mathcal{F}}_G$ is the *one-dimensional* Fourier transform given by

$$\tilde{\mathcal{F}}_G(k) = \frac{1}{2\pi}\int_{-\infty}^{\infty} G(r)e^{-ikr}dr. \tag{B9}$$

Using this equation, we have calculated the Fourier transforms given in Table VI for a variety of important operators in quantum chemical theories, including those used in this work. In each case, the transforms are easily seen to fulfill the necessary conditions and the Schwarz inequality holds for each of these operators.

[1] J. L. Whitten, J. Chem. Phys. **58**, 4496 (1973).
[2] M. Häser and R. Ahlrichs, J. Comput. Chem. **10**, 104 (1989).
[3] S. A. Maurer, D. S. Lambrecht, D. Flaig, and C. Ochsenfeld, J. Chem. Phys. **136**, 144107 (2012).
[4] D. S. Hollman, H. F. Schaefer, and E. F. Valeev, J. Chem. Phys. **142**, 154106 (2015).
[5] M. Beuerle, J. Kussmann, and C. Ochsenfeld, J. Chem. Phys. **146**, 144108 (2017).
[6] C. Hättig, W. Klopper, A. Köhn, and D. P. Tew, Chem. Rev. **112**, 4 (2012).
[7] L. Kong, F. A. Bischoff, and E. F. Valeev, Chem. Rev. **112**, 75 (2012).
[8] J. Heyd, G. E. Scuseria, and M. Ernzerhof, J. Chem. Phys. **118**, 8207 (2003).
[9] S. Ten-no, Chem. Phys. Lett. **398**, 56 (2004).
[10] K. A. Peterson, T. B. Adler, and H. J. Werner, J. Chem. Phys. **128**, 084102 (2008).
[11] A. V. Krukau, O. A. Vydrov, A. F. Izmaylov, and G. E. Scuseria, J. Chem. Phys. **125**, 224106 (2006).
[12] J. G. Brandenburg, E. Caldeweyher, and S. Grimme, Phys. Chem. Chem. Phys. **18**, 15519 (2016).
[13] R. Peverati and D. G. Truhlar, Phys. Chem. Chem. Phys. **14**, 16187 (2012).
[14] J. Kussmann, M. Beer, and C. Ochsenfeld, Wiley Interdiscip. Rev.: Comput. Mol. Sci. **3**, 614 (2013).
[15] C. A. White, B. G. Johnson, P. M. Gill, and M. Head-Gordon, Chem. Phys. Lett. **230**, 8 (1994).
[16] E. Schwegler, M. Challacombe, and M. Head-Gordon, J. Chem. Phys. **106**, 9708 (1997).
[17] C. Ochsenfeld, C. A. White, and M. Head-Gordon, J. Chem. Phys. **109**, 1663 (1998).
[18] C. Ochsenfeld, Chem. Phys. Lett. **327**, 216 (2000).
[19] H.-A. Le and T. Shiozaki, e-print arXiv:1708.05353v1 (2017).
[20] J. Kussmann and C. Ochsenfeld, J. Chem. Phys. **138**, 134114 (2013).
[21] C. C. J. Roothaan, Rev. Mod. Phys. **23**, 69 (1951).
[22] T. Helgaker, P. Jorgensen, and J. Olsen, *Molecular Electronic-Structure Theory* (Wiley, 2000), pp. 431–432.
[23] E. H. Lieb and M. Loss, *Analysis*, 2nd ed. (American Mathematical Society, 2001).
[24] E. H. Lieb and R. Seiringer, *The Stability of Matter in Quantum Mechanics* (Cambridge University Press, 2010).
[25] J. Heyd and G. E. Scuseria, J. Chem. Phys. **121**, 1187 (2004).
[26] T. B. Adler, H.-J. Werner, and F. R. Manby, J. Chem. Phys. **130**, 054106 (2009).
[27] S. Bochner, *Lectures on Fourier Integrals* (Princeton University Press, 1959).
[28] L. Grafakos and G. Teschl, J. Fourier Anal. Appl. **19**, 167 (2013).